1

Basic Mean-Field Theory for Bose–Einstein Condensates

P.G. Kevrekidis, D.J. Frantzeskakis, and R. Carretero-González

1.1 Introduction

The phenomenon of Bose–Einstein condensation, initially predicted by Bose [1] and Einstein [2, 3] in 1924, refers to systems of particles obeying the Bose statistics. In particular, when a gas of bosonic particles is cooled below a critical transition temperature T_c, the particles merge into the Bose–Einstein condensate (BEC), in which a macroscopic number of particles (typically 10^3 to 10^6) share the same quantum state. Bose–Einstein condensation is in fact a quantum phase transition, which is connected to the manifestation of fundamental physical phenomena, such as superfluidity in liquid helium and superconductivity in metals (see, e.g., [4] for a relevant discussion and references). Dilute weakly-interacting BECs were first realized experimentally in 1995 in atomic gases, and specifically in vapors of rubidium [5] and sodium [6]. In the same year, first signatures of Bose–Einstein condensation in vapors of lithium were also reported [7] and were later more systematically confirmed [8]. The significance and importance of the emergence of BECs has been recognized through the 2001 Nobel prize in Physics [9, 10]. During the last years there has been an explosion of interest in the physics of BECs. Today, over fifty experimental groups around the world can routinely produce BECs, while an enormous amount of theoretical work has ensued.

From a theoretical standpoint, and for a wide range of experimentally relevant conditions, the dynamics of a BEC can be described by means of an effective mean-field theory. This approach is much simpler than treating the full many-body Schrödinger equation and can describe quite accurately the static and dynamical properties of BECs. The relevant model is a classical nonlinear evolution equation, the so-called Gross–Pitaevskii (GP) equation [11, 12]. In fact, this is a variant of the famous nonlinear Schrödinger (NLS) equation [13], which is a universal model describing the evolution of complex field envelopes in nonlinear dispersive media. The NLS is widely relevant to other areas of applications ranging from optics to fluid dynamics and plasma physics [14], while it is also interesting from a mathematical viewpoint [13–15]. In the case

of BECs, the nonlinearity in the GP model is introduced by the interatomic interactions, accounted for through an effective mean-field. Importantly, the study of the GP equation allows the prediction and description of important, and experimentally relevant, nonlinear effects and nonlinear states (such as solitons and vortices), which constitute the subject of this book.

This chapter is devoted to the mean-field description of BECs, the GP model and its properties. In particular, we present the derivation of the GP equation (see also Chap. 18) and some of its basic features. We discuss the different cases of repulsive and attractive interatomic interactions and how to control them via Feshbach resonances. We describe the external potentials that can be used to confine BECs, as well as how their form leads to specific types of simplified mean-field descriptions. Finally, we discuss the ground state properties of BECs and their small-amplitude excitations.

1.2 The Gross–Pitaevskii (GP) Mean-Field Model

1.2.1 Origin and Basic Properties of the GP Equation

The many-body Hamiltonian for N interacting bosons of mass m confined by an external potential $V_{\rm ext}(\mathbf{r})$ is given in second quantization form by [16–18]

$$\begin{aligned}\hat{H} &= \int \mathrm{d}\mathbf{r}\hat{\Psi}^\dagger(\mathbf{r})\left[-\frac{\hbar^2}{2m}\nabla^2 + V_{\rm ext}(\mathbf{r})\right]\hat{\Psi}(\mathbf{r}) \\ &\quad + \frac{1}{2}\int \mathrm{d}\mathbf{r}\,\mathrm{d}\mathbf{r}'\hat{\Psi}^\dagger(\mathbf{r})\hat{\Psi}^\dagger(\mathbf{r}')V(\mathbf{r}-\mathbf{r}')\hat{\Psi}(\mathbf{r}')\hat{\Psi}(\mathbf{r}), \qquad (1.1)\end{aligned}$$

where $\hat{\Psi}(\mathbf{r})$ and $\hat{\Psi}^\dagger(\mathbf{r})$ are the boson annihilation and creation field operators respectively, and $V(\mathbf{r}-\mathbf{r}')$ is the two-body interatomic potential. Adopting the well-established mean-field approximation [16–20], we use the decomposition $\hat{\Psi}(\mathbf{r},t) = \Psi(\mathbf{r},t) + \hat{\Psi}'(\mathbf{r},t)$. In this expression, the complex function $\Psi(\mathbf{r},t) \equiv \langle\hat{\Psi}(\mathbf{r},t)\rangle$ (i.e., the expectation value of the field operator), has the meaning of an *order parameter* and is commonly known as the *macroscopic wavefunction of the condensate*. On the other hand, $\hat{\Psi}'(\mathbf{r}',t)$ describes the non-condensate part, which, at temperatures well below $T_{\rm c}$, it is reasonable to assume that it is negligible (for a more formal and complete discussion please refer to Chap. 18). Then, the above prescription leads to a nontrivial zeroth-order theory for the BEC wavefunction as follows: First, from the Heisenberg equation $\mathrm{i}\hbar(\partial\hat{\Psi}/\partial t) = [\hat{\Psi}, \hat{H}]$ for the field operator $\hat{\Psi}(\mathbf{r},t)$, we obtain

$$\mathrm{i}\hbar\frac{\partial}{\partial t}\hat{\Psi}(\mathbf{r},t) = \left[-\frac{\hbar^2}{2m}\nabla^2 + V_{\rm ext}(\mathbf{r}) + \int \mathrm{d}\mathbf{r}'\hat{\Psi}^\dagger(\mathbf{r}',t)V(\mathbf{r}'-\mathbf{r})\hat{\Psi}(\mathbf{r}',t)\right]\hat{\Psi}. \quad (1.2)$$

The next step is to simplify the interatomic interaction potential, $V(\mathbf{r}'-\mathbf{r})$. Consider the relevant case of a dilute ultracold gas with binary collisions at low energy, characterized by the s-wave scattering length a. In this limit, it can

be shown [16–18,20] (see also Chap. 18) that the interatomic potential can be replaced by an effective interaction which is well described by a delta-function potential, $V(\mathbf{r}' - \mathbf{r}) = g\delta(\mathbf{r}' - \mathbf{r})$, where the coupling constant g is given by $g = 4\pi\hbar^2 a/m$. Employing this effective interaction potential and replacing the field operator $\hat{\Psi}$ with the classical field Ψ, (1.2) yields the GP equation,

$$\mathrm{i}\hbar\frac{\partial}{\partial t}\Psi(\mathbf{r},t) = \left[-\frac{\hbar^2}{2m}\nabla^2 + V_{\mathrm{ext}}(\mathbf{r}) + g|\Psi(\mathbf{r},t)|^2\right]\Psi(\mathbf{r},t). \tag{1.3}$$

The complex function Ψ in the GP (1.3) can be expressed in terms of the density $n(\mathbf{r},t) \equiv |\Psi(\mathbf{r},t)|^2$, and phase $S(\mathbf{r},t)$ of the condensate as $\Psi(\mathbf{r},t) = \sqrt{n(\mathbf{r},t)}\exp\left[\mathrm{i}S(\mathbf{r},t)\right]$. Note that the phase $S(\mathbf{r},t)$ fixes the atomic velocity as follows: The current density $\mathbf{j} = \frac{\hbar}{2m\mathrm{i}}(\Psi^\star\nabla\Psi - \Psi\nabla\Psi^\star)$ (where star denotes complex conjugate), assumes a hydrodynamic form $\mathbf{j} = n\mathbf{v}$, with atomic velocity $\mathbf{v}(\mathbf{r},t) = \frac{\hbar}{m}\nabla S(\mathbf{r},t)$. This indicates that the atomic velocity is irrotational, i.e., $\nabla\times\mathbf{v} = 0$, which is a typical characteristic of *superfluids*. A detailed description on the hydrodynamics approach for the BEC superfluid can be found in Chap. 11.

The GP model conserves the total number of atoms, N, given by

$$N = \int |\Psi(\mathbf{r},t)|^2 \mathrm{d}\mathbf{r}. \tag{1.4}$$

On the other hand, (1.3) can be written in canonical form, $\mathrm{i}\hbar\frac{\partial}{\partial t}\Psi = \frac{\delta E}{\delta\Psi^\star}$, where the dynamically conserved energy functional E is given by

$$E = \int \mathrm{d}\mathbf{r}\left[\frac{\hbar^2}{2m}|\nabla\Psi|^2 + V_{\mathrm{ext}}|\Psi|^2 + \frac{1}{2}g|\Psi|^4\right] \tag{1.5}$$

with the three terms in the right-hand side representing, respectively, the kinetic energy, the potential energy and the interaction energy. Equations (1.4) and (1.5) indicate that the GP equation possesses two integrals of motion, the number of atoms N and the energy of the system E (provided, of course, that the external potential, V_{ext}, is time independent).

1.2.2 Repulsive and Attractive Interactions: Feshbach Resonance

The coefficient g which sets the nonlinearity strength in the GP (1.3), may take either positive or negative values; this is due to the fact that the scattering length may be $a > 0$ (e.g., for rubidium or sodium BEC) or $a < 0$ (e.g., for lithium BEC). The two cases correspond, respectively, to repulsive and attractive interactions between the atoms, or to defocusing and focusing Kerr-type nonlinearities in the language of nonlinear optics [13,21].

Importantly, it is possible to control the interatomic interaction by changing the threshold collision dynamics, and consequently change the sign or the magnitude of the scattering length. This can be done upon applying an

external magnetic field, B, which controls the scattering length because of the rapid variation in collision properties associated with a threshold scattering resonance being a *Feshbach resonance* (see, e.g., [22] for the theoretical aspects, as well as [23, 24] and [25, 26] for relevant experimental results for sodium and rubidium condensates respectively). Specifically, the behavior of the scattering length near a Feshbach resonant magnetic field B_0 is typically of the form [27, 28],

$$a(B) = \tilde{a}\left(1 - \frac{\Delta}{B - B_0}\right), \tag{1.6}$$

where $\tilde{a}$ is the value of the scattering length far from resonance and Δ represents the width of the resonance. On the other hand, a complementary way of tuning the scattering length can be achieved in low-dimensional setups (cf. Sect. 1.3). The extreme case of a very strong transversal confinement results in the so-called *confinement induced resonance*, at which the modified scattering length diverges [29, 30]. A third alternative approach uses the possibility of tuning the scattering length with an *optically induced Feshbach resonance* [31].

The possibility of the control over the interactions and collisional properties of the atoms was crucial for a variety of experimental discoveries such as the formation of bright matter-wave solitons [32–35], the formation of molecular BECs [36–38], and the revelation of the BEC–BCS (Bardeen–Cooper–Schrieffer) crossover [39, 40].

1.2.3 The External Potential

The external potential $V_{\text{ext}}(\mathbf{r})$ in the GP (1.3) can assume different forms, depending on the type of trapping, i.e., magnetic or optical. In particular, while in the first experiments BECs were confined by means of magnetic fields [9, 10, 16–18], later on the BEC confinement in purely optical fields became also possible. The first purely optical confinement of BECs was achieved in 1998 [41], where the condensate was first created in a magnetic trap and then was loaded into the optical dipole trap (see, e.g., relevant reviews in [42, 43]). However, from a 2001 experiment [44] it was demonstrated that it is possible to directly create and confine BECs in an optical dipole trap. The advantage of the optical dipole traps is that their shape is extremely flexible and controllable. An example of such control is a special case of optical potentials called optical lattices, in which the light field is a standing wave; in such a case, the resulting dipole potential is a crystal-like lattice of potential wells. Part VIII presents a detailed description on the theoretical and experimental aspects of optical lattices. In the first relevant experiments of [45, 46], cold atoms were trapped in optical lattices tuned close to resonance (i.e., the laser frequency was close to the atomic transition frequency); as a result, an effective dissipative behavior was observed due to the fact that spontaneous emission dominated the dipole trapping force. However, in

1996, non-dissipative far off-resonant optical lattices were first used to trap laser-cooled atoms [47]. Such far-detuned optical lattice potentials have been useful in elucidating novel physical phenomena in BECs (see, e.g., the recent review [48]).

In the case of the "standard" magnetic trap the external potential assumes the typical harmonic form:

$$V_{\rm MT}(\mathbf{r}) = \frac{1}{2}m(\omega_x^2 x^2 + \omega_y^2 y^2 + \omega_z^2 z^2), \tag{1.7}$$

where, in general, the trap frequencies $\omega_x, \omega_y, \omega_z$ along the three directions are different. As a result, the geometry of the trap and, hence, the shape of the condensate itself, may range from isotropic forms, to strongly anisotropic ones. In particular, if $\omega_x = \omega_y \equiv \omega_r \approx \omega_z$ the trap is isotropic and the BEC is almost spherical, while the cases $\omega_z < \omega_r$ or $\omega_r < \omega_z$ describe anisotropic traps in which the BEC is, respectively, elongated, "cigar shaped", or flattened, "pancake-shaped". The latter anisotropic cases, and especially the strongly anisotropic ones ($\omega_z \ll \omega_r$ or $\omega_r \ll \omega_z$), are particularly interesting as they are connected to effectively lower dimensional BECs, namely quasi one-dimensional (1D) and quasi two-dimensional (2D), respectively. At temperatures close to zero where phase fluctuations are negligible such *weakly-interacting* 1D and 2D condensates are possible (see a relevant discussion in Chap. 18), and have been realized experimentally in optical and magnetic traps [49], in optical lattice potentials [50–55], as well as surface microtraps [56, 57] (see also the recent review [58] for a relevant rigorous mathematical analysis). In this context, it is worth mentioning that even the limiting case of the purely 1D, *strongly-interacting*, so-called, Tonks–Girardeau gas [59, 60] (in which the interacting bosonic gas behaving like a system of free fermions) has recently been observed experimentally [61, 62].

On the other hand, as mentioned above, the optical lattice is imposed by a pair of laser beams forming a standing wave which generates a periodic potential. For example, a single periodic 1D standing wave of the form $E(z,t) = 2E_0 \cos(kz)\exp(-\mathrm{i}\omega t)$ can be created by the superposition of the two identical beams, $E_\pm(z,t) = E_0 \exp[\mathrm{i}(\pm kz - \omega t)]$, having the same polarization, amplitude E_0, wavelength $\lambda = 2\pi/k$, and frequency ω. Since the dipole potential $V_{\rm dip}$ is proportional to the intensity $I \sim |E(z,t)|^2$ of the light field [43], this leads to a periodic potential, i.e., an optical lattice of the form $V_{\rm dip} \equiv V_{\rm OL} = V_0 \cos^2(kz)$. In such a case, the lattice periodicity is $\lambda/2$ and the lattice height is given by $V_0 \sim I_{\max}/\Delta\omega$, where $I_{\max}$ is the maximum intensity of the light field and $\Delta\omega \equiv \omega - \omega_{\rm o}$ is the detuning of the lasers from the atomic transition frequency $\omega_{\rm o}$. Note that atoms are trapped in the nodes (anti-nodes) of the optical lattice for blue- (red-) detuned laser beams, or $\Delta\omega > 0$ ($\Delta\omega < 0$). In a more general, three-dimensional (3D) setting, the optical lattice potential can take the following form:

$$V_{\rm OL}(\mathbf{r}) = V_0 \left[\cos^2(k_x x + \phi_x) + \cos^2(k_y y + \phi_y) + \cos^2(k_z z + \phi_z)\right], \tag{1.8}$$

where $k_i = 2\pi/\lambda_i$ ($i \in \{x, y, z\}$), $\lambda_i = \lambda/[2\sin(\theta_i/2)]$, θ_i are the (potentially variable) angles between the laser beams [48] (see also [63] and Part VIII) and ϕ_i are arbitrary phases.

It is also possible to realize experimentally an "optical superlattice", characterized by two different periods. In particular, as demonstrated in [64], such an optical superlattice can be formed by the sequential creation of two lattice structures using four laser beams. A stationary 1D superlattice can be described as $V(z) = V_1 \cos(k_1 z) + V_2 \cos(k_2 z)$, where k_i, V_i denote, respectively, the wavenumbers and amplitudes of the sublattices. The experimental tunability of these parameters provides precise and flexible control over the shape and time-variation of the external potential.

It is worth mentioning that the magnetic or/and the optical dipole traps can be experimentally combined either together, or with other potentials; an example is far off-resonant laser beams, that can create effective repulsive potential barriers (for blue-detuned lasers) or attractive localized potentials (for red-detuned lasers). An important example of such a combination of a harmonic trap with a repulsive potential located at the center of the harmonic trap is the *double-well* potential. Such a potential has been used in the seminal interference experiment of [65], which demonstrated that BECs are in fact coherent matter-waves. Double-well potentials have also been created by a combination of a harmonic and a periodic optical potential [66]. Finally, other combinations, including, e.g., linear ramps of (gravitational) potential $V_{\rm ext} = mgz$ have also been experimentally applied (see, e.g., [66, 67]). Additional recent possibilities include the design and implementation of external potentials, offered e.g., by the so-called *atom chips* [56, 57, 68, 69]. Generally, nowadays there exists a major flexibility for the creation of a wide variety of shapes and types (e.g., stationary, time-dependent, etc.) of external potentials.

1.3 Dimensionality Reduction

1.3.1 Length Scales

The confining frequencies ω_j ($j \in \{x, y, z\}$) of the magnetic trapping potential set characteristic length scales for the spatial size of the condensate through the characteristic harmonic oscillator lengths $a_{{\rm ho},j} \equiv (\hbar/m\omega_j)^{1/2}$. Another important length scale, introduced by the effective mean-field nonlinearity, is the so-called "healing length" [16–18], which is the distance over which the kinetic energy and the interaction energy balance: if the BEC density grows from 0 to n over the distance ξ, the kinetic energy, $\sim\hbar^2/(2m\xi^2)$, and interaction energy, $\sim 4\pi\hbar^2 an/m$, become equal at the value of ξ given by

$$\xi = (8\pi na)^{-1/2}. \tag{1.9}$$

Note that the name of ξ is coined by the fact that it is actually the distance over which the BEC wavefunction Ψ "heals" over defects. Thus, the spatial widths of nonlinear excitations, such as dark solitons and vortices in BECs, are of $\mathrm{O}(\xi)$.

1.3.2 Derivation of Lower-Dimensional Models

Let us assume that $\omega_x = \omega_y \equiv \omega_r$. Then, if the transverse harmonic oscillator length $a_{\mathrm{ho},r} \equiv \sqrt{\hbar/m\omega_r} < \xi$, the transverse confinement of the condensate is so tight that the dynamics of such a cigar-shaped BEC can be considered to be effectively 1D. This allows for a reduction of the fully 3D GP equation to an effectively 1D GP model, which can be done for sufficiently small trapping frequency ratios ω_z/ω_r. It should be stressed, however, that such a reduction should be only considered as the 1D limit of a 3D mean-field theory and *not* as a genuine 1D theory (see, e.g., [58] for a relevant discussion). Similar considerations also hold for a pancake-shaped BEC, for which the condition $a_{\mathrm{ho},z} < \xi$ along with the requirement of sufficiently small frequency ratios ω_r/ω_z, allows for a reduction to an effective 2D GP model. Such a reduction can be done following the same procedure as in the quasi-1D setting; thus, below we will confine ourselves to cigar-shaped BECs.

In the quasi-1D setting, assuming a highly anisotropic trap with $\omega_z \ll \omega_\perp \equiv \omega_x = \omega_y$, we may decompose the wavefunction Ψ in a longitudinal (along z) and a transverse [on the (x, y) plane] component, and seek for solutions of (1.3) in the form

$$\Psi(\mathbf{r}, t) = \psi(z, t)\, \Phi(r) \exp(-\mathrm{i}\gamma t), \tag{1.10}$$

where $r^2 \equiv x^2 + y^2$, while the chemical potential γ and the transverse wavefunction $\Phi(r)$ are involved in the auxiliary problem for the transverse quantum harmonic oscillator,

$$\frac{\hbar^2}{2m}\nabla_\perp^2 \Phi - \frac{1}{2} m\omega_r^2 r^2 \Phi + \gamma\Phi = 0, \tag{1.11}$$

where $\nabla_\perp^2 \equiv \partial^2/\partial x^2 + \partial^2/\partial y^2$. Since the considered system is effectively 1D, it is natural to assume that the transverse component of the condensate wavefunction $\Phi(r)$ remains in the ground state; in such a case $\Phi(r)$ takes the form $\Phi(r) = \pi^{-1/2} a_r^{-1} \exp(-r^2/2a_r^2)$ [when considering the reduction from 3D to 2D the transverse wave function reduces to $\Phi(r) = \pi^{-1/4} a_r^{-1/2} \exp(-r^2/2a_r^2)$]. Then, substituting (1.10) into (1.3) and averaging the resulting equation in the r-direction (i.e., multiplying by $\Phi^\star = \Phi$ and integrating with respect to r), we finally obtain the following 1D GP equation,

$$\mathrm{i}\hbar\frac{\partial}{\partial t}\psi(z, t) = \left[-\frac{\hbar^2}{2m}\frac{\partial^2}{\partial z^2} + V(z) + \tilde{g}|\psi(z, t)|^2\right]\psi(z, t), \tag{1.12}$$

where the new coupling constant $\tilde{g}$ has an effective 1D form, namely $\tilde{g} = g/2\pi a_r^2 = 2a\hbar\omega_r$ and $V(z) = (1/2)m\omega_z^2 z^2$.

A similar reduction can be performed if, additionally, an optical lattice potential is present. In fact, it is possible (as, e.g., in the experiment in [70]) to tune ω_z so that it provides only a very weak trapping along the z-direction; in this way the shift in the potential trapping energies over the wells where the condensate is confined can be made practically negligible. In such a case, the potential in (1.12) is simply the 1D optical lattice $V(z) = V_0 \cos^2(kz)$. Similar considerations can be done e.g., in the quasi-2D case, introducing an "egg-carton potential" $V(x,y) = V_0 \left[\cos^2(k_x x) + \cos^2(k_y y)\right]$ for pancake-shaped condensates. We note in passing that dimensionality reduction techniques, such as the averaging method discussed above, are commonly used in other disciplines, e.g., in nonlinear fiber optics [21].

In the BEC context, apart from the above averaging method [71–73] (see also [74]), reduction of the 3D GP equation to 1D can be done self-consistently, using a multiscale expansion technique [75, 76], a variational approach [77] and other methods [78]. Importantly, many experimental results have been effectively described by lower dimensional GP models, also ones exhibiting *non-polynomial* nonlinearities [77] (see, e.g., the recent experiment [66]). It is relevant to note that lower-dimensional GP models with a *cubic-quintic* nonlinearity (that can also be obtained by Taylor expanding the non-polynomial nonlinearity of [77]) have been also been employed in various studies (see, e.g., [78–82]).

1.3.3 The Discrete Nonlinear Schrödinger Equation

Another useful reduction, which is relevant to deep optical lattice potentials, so that the chemical potential $\mu \ll V_0$ (see Sec. 1.4), is the one of the GP equation to a genuinely discrete model, the so-called *discrete NLS* (DNLS) equation [83]. Such a reduction has been introduced in the context of arrays of BEC droplets confined in the wells of an optical lattice in [84,85] and further elaborated in [86]; we will follow the latter below. For convenience, we first use characteristic units, based on the lattice (and atomic) parameters, provided by the length k^{-1} (where $k = 2\pi/\lambda$ is the optical lattice wavenumber) and the recoil energy $E_{\rm rec} = \hbar^2 k^2/2m$ (i.e., the kinetic energy gained by an atom when it absorbs a photon from the optical lattice), to express (1.12) in the following dimensionless form:

$$\mathrm{i}\frac{\partial}{\partial t}\psi(z,t) = \left[-\frac{\partial^2}{\partial z^2} + V(z) + g|\psi(z,t)|^2\right]\psi(z,t). \tag{1.13}$$

In (1.13), length is scaled in units of k^{-1}, time in units of $\hbar/E_{\rm rec}$, the atomic density $|\psi|^2$ is rescaled in units of $(\pi^2/a)(a_r/\lambda)^2$, and energy is measured in units of the recoil energy. Finally, the coupling constant g in (1.13) is rescaled

to unity, i.e., $g = \pm 1$ for repulsive and attractive interatomic interactions respectively.

Next, assuming that $V(z)$ in (1.13) is a general periodic potential, i.e., $V(z+L) = V(z)$, we consider the eigenvalue problem associated to (1.13),

$$\frac{\mathrm{d}^2\varphi_{k,\alpha}}{\mathrm{d}z^2} + V(z)\varphi_{k,\alpha} = E_\alpha(k)\varphi_{k,\alpha}, \tag{1.14}$$

where $\varphi_{k,\alpha}$ has Bloch (Floquet) functions $\varphi_{k,\alpha} = \exp(\mathrm{i}kx)\psi_{k,\alpha}(x)$, with $\psi_{k,\alpha}(x)$ being periodic with period L [α is an index labeling the energy bands $E_\alpha(k)$]. It is then useful to employ the (localized in each well of the optical lattice) Wannier functions [87], i.e., the Fourier transform of the Bloch functions. Due to the completeness of the Wannier basis, any solution of (1.13) can be expressed in the form $\psi(x,t) = \sum_{n,\alpha} c_{n,\alpha}(t) w_{n,\alpha}(x)$. Substituting the above expression into (1.13), and using the orthonormality of the Wannier basis, we obtain a set of differential equations for the coefficients [depending on the well (n) and band (α) index]. Upon suitable decay of the Fourier coefficients and the Wannier functions' prefactors (which can be systematically checked for given potential parameters), the model can then be reduced to

$$\begin{aligned} \mathrm{i}\frac{\mathrm{d}c_{n,\alpha}}{\mathrm{d}t} = {} & \hat{\omega}_{0,\alpha} c_{n,\alpha} + \hat{\omega}_{1,\alpha}\left(c_{n-1,\alpha} + c_{n+1,\alpha}\right) \\ & + g \sum_{\alpha_1,\alpha_2,\alpha_3} W^{nnnn}_{\alpha\alpha_1\alpha_2\alpha_3} c^*_{n,\alpha_1} c_{n,\alpha_2} c_{n,\alpha_3}, \end{aligned} \tag{1.15}$$

where $W^{nn_1n_2n_3}_{\alpha\alpha_1\alpha_2\alpha_3} = \int_{-\infty}^{\infty} w_{n,\alpha} w_{n_1,\alpha_1} w_{n_2,\alpha_2} w_{n_3,\alpha_3} \mathrm{d}x$. The latter equation degenerates into the tight-binding model [84, 85],

$$\mathrm{i}\frac{\mathrm{d}c_{n,\alpha}}{\mathrm{d}t} = \hat{\omega}_{0,\alpha} c_{n,\alpha} + \hat{\omega}_{1,\alpha}\left(c_{n-1,\alpha} + c_{n+1,\alpha}\right) + g W^{nnnn}_{1111} |c_{n,\alpha}|^2 c_{n,\alpha}, \tag{1.16}$$

if one restricts consideration only to the first band. Equation (1.16) is precisely the reduction of the NLS to its discrete counterpart: the discrete NLS (DNLS).

1.4 Ground State and Excitations

1.4.1 Ground State

The ground state of the GP model of (1.3) can readily be found upon expressing the condensate wave function as $\Psi(\mathbf{r},t) = \Psi_0(\mathbf{r})\exp(-\mathrm{i}\mu t/\hbar)$, where Ψ_0 is a real function (normalized to the number of atoms, $\int \mathrm{d}\mathbf{r}\, \Psi_0^2 = N$) and $\mu = \partial E/\partial N$ is the chemical potential. Substitution of the above expression into (1.3) yields the following steady-state equation for Ψ_0:

$$\left[-\frac{\hbar^2}{2m}\nabla^2 + V_{\mathrm{ext}}(\mathbf{r}) + g\Psi_0^2(\mathbf{r})\right]\Psi_0(\mathbf{r}) = \mu\Psi_0(\mathbf{r}). \tag{1.17}$$

If $g = 0$, (1.17) reduces to the usual Schrödinger equation with potential $V_{\rm ext}$. Then, for a harmonic external trapping potential [see (1.7)], the ground state of the system is obtained when letting all non-interacting bosons occupy the lowest single-particle state; there, Ψ_0 has the Gaussian profile

$$\Psi_0(\mathbf{r}) = \sqrt{N}\left(\frac{m\omega_{\rm ho}}{\pi\hbar}\right)^{3/4} \exp\left[-\frac{m}{2\hbar}(\omega_x^2 x^2 + \omega_y^2 y^2 + \omega_z^2 z^2)\right], \tag{1.18}$$

where $\omega_{\rm ho} = (\omega_x\omega_y\omega_z)^{1/3}$ is the geometric average of the confining frequencies.

For repulsive interatomic forces ($g > 0$, or scattering length $a > 0$), if the number of atoms of the condensate is sufficiently large so that $Na/a_{\rm ho} \gg 1$, the atoms are pushed towards the rims of the condensate, resulting in slow spatial variations of the density. Then the kinetic energy (gradient) term is very small compared to the interaction and potential energies and becomes significant only close to the boundaries. Thus, the Laplacian kinetic energy term in (1.17) can safely be neglected. This results in the, so-called, Thomas–Fermi (TF) approximation [16–18] for the system's ground state density profile:

$$n(\mathbf{r}) = |\Psi_0(\mathbf{r})|^2 = g^{-1}\left[\mu - V_{\rm ext}(\mathbf{r})\right], \tag{1.19}$$

in the region where $\mu > V_{\rm ext}(\mathbf{r})$, and $n = 0$ outside. In this approximation, for a spherically symmetric harmonic magnetic trap ($V_{\rm ext} = V_{\rm MT}$ with $\omega_{\rm ho} = \omega_x = \omega_y = \omega_z$), the radius $R_{\rm TF} = (2\mu/m)^{1/2}/\omega_{\rm ho}$ for which $n(R_{\rm TF}) = 0$, the so-called Thomas–Fermi radius, determines the size of the condensed cloud. Furthermore, the normalization condition connects μ and N through the equation $\mu = (\hbar\omega_{\rm ho}/2)(15Na/a_{\rm ho})^{2/5}$.

For attractive interatomic forces ($g < 0$, or $a < 0$), the density tends to increase at the trap center, while the kinetic energy tends to balance this increase. However, if the number of atoms N in the condensate exceeds a critical value, i.e., $N > N_{\rm cr}$, the system is subject to *collapse* in a 2D or a 3D setting, respectively [13, 17, 18]. Collapse was observed experimentally in both cases of the attractive ^{7}Li [88] and ^{85}Rb condensate [89]. The critical number of atoms necessary for collapse in a spherical BEC is determined by the equation [90], $N_{\rm cr}|a|/a_{\rm ho} = 0.575$, where $|a|$ is the absolute value of the scattering length and $a_{\rm ho} = (\hbar/m\omega_{\rm ho})^{1/2}$. Importantly, collapse may not occur in a quasi-1D setting, which implies that cigar-shaped attractive BECs (confined in a trap with frequencies $\omega_z \ll \omega_r$) are not subject to collapse, provided that their number of atoms does not exceed the critical value given by the equation $N_{\rm cr}|a|/a_{{\rm ho},r} = 0.676$, with $a_{{\rm ho},r}$ being the transverse harmonic oscillator length [71, 91, 92].

1.4.2 Small-Amplitude Linear Excitations

Let us now consider small-amplitude excitations of the condensate, which can be found in the framework of mean-field theory upon linearizing the

time-dependent GP equation around the ground state. Specifically, solutions of (1.3) can be sought in the form

$$\Psi(\mathbf{r},t) = \mathrm{e}^{-\mathrm{i}\mu t/\hbar}\left[\Psi_0(\mathbf{r}) + \sum_j \left(u_j(\mathbf{r})\mathrm{e}^{-\mathrm{i}\omega_j t} + \upsilon_j^\star(\mathbf{r})\mathrm{e}^{\mathrm{i}\omega_j^\star t}\right)\right], \tag{1.20}$$

where u_j, υ_j are small (generally complex) perturbations, describing the components of the condensate's (linear) response to the external perturbations that oscillate at frequencies $\pm\omega_j$ [the latter are (generally complex) eigenfrequencies]. Substituting (1.20) into (1.3), and keeping only the linear terms in u_j and υ_j, the following set of equations is derived

$$\begin{aligned}\left[\hat{H}_0 - \mu + 2g\,\Psi_0^2(\mathbf{r})\right] u_j(\mathbf{r}) + g\,\Psi_0^2(\mathbf{r})\upsilon_j(\mathbf{r}) &= \hbar\,\omega_j\,u_j(\mathbf{r}),\\ \left[\hat{H}_0 - \mu + 2g\,\Psi_0^2(\mathbf{r})\right] \upsilon_j(\mathbf{r}) + g\,\Psi_0^{\star 2}(\mathbf{r})u_j(\mathbf{r}) &= -\hbar\,\omega_j\,\upsilon_j(\mathbf{r}),\end{aligned} \tag{1.21}$$

where $\hat{H}_0 \equiv -(\hbar^2/2m)\nabla^2 + V_{\mathrm{ext}}(\mathbf{r})$. Equations (1.21) are known as the *Bogoliubov–de Gennes (BdG) equations*. These equations can also be derived using a purely quantum-mechanical approach [16–18, 20] and can be used, apart from the case of the ground state, for other states (such as solitons and vortices) with the function Ψ_0 being modified accordingly.

The BdG equations are intimately connected to the stability of the state Ψ_0. Specifically, suitable combinations of (1.21) yield

$$(\omega_j - \omega_j^\star)\int(|u_j|^2 - |\upsilon_j|^2)\mathrm{d}\mathbf{r} = 0. \tag{1.22}$$

Equation (1.22) can be satisfied in two different ways: First, if $\omega_j - \omega_j^\star = 0$, i.e., if the eigenfrequencies ω_j are real; in that case, the fact that $\mathrm{Im}\{\omega_j\} = 0$ shows that the state Ψ_0 is *stable*. Note that, in this case, one can use the normalization condition for the eigenmodes u_j, υ_j of the form $\int(|u_j|^2 - |\upsilon_j|^2)\,\mathrm{d}\mathbf{r} = 1$. Alternatively, occurrence of complex eigenfrequencies ω_j (i.e., if $\omega_j - \omega_j^\star \neq 0$ or $\mathrm{Im}\{\omega_j\} \neq 0$), indicates *dynamical instability* of the state Ψ_0; in such a case, (1.22) is satisfied only if $\int|u_j|^2\mathrm{d}\mathbf{r} = \int|\upsilon_j|^2\mathrm{d}\mathbf{r}$.

The BdG equations provide interesting results even in the case of a uniform gas ($V_{\mathrm{ext}}(\mathbf{r}) = 0$). In such a case, the amplitudes u and υ are plane waves $\sim\mathrm{e}^{\mathrm{i}\mathbf{k}\cdot\mathbf{r}}$ (of wavevector $\mathbf{k}$) and (1.21) lead to a dispersion relation, known as the *Bogoliubov spectrum*:

$$(\hbar\omega)^2 = \left(\frac{\hbar^2\mathbf{k}^2}{2m}\right)\left(\frac{\hbar^2\mathbf{k}^2}{2m} + 2gn\right). \tag{1.23}$$

For small momenta $\hbar k$, (1.23) yields the phonon dispersion relation $\omega = cq$, where $c = \sqrt{gn/m}$ is the speed of sound. On the other hand, for large momenta, the spectrum provides the free particle energy $\hbar^2k^2/(2m)$, with

the "crossover" between the two regimes occurring when the excitation wavelength is of the order of the healing length given by (1.9).

Finally, it should be noticed that in the case of attractive interatomic interactions $g < 0$, the speed of sound becomes imaginary, which indicates that long wavelength perturbations grow or decay exponentially in time. This effect is directly connected to the *modulational instability*, which leads to delocalization in momentum space and, in turn, to localization in position space and the formation of solitary-wave structures. The effect of modulational instability is responsible for the formation of bright matter-wave solitons [32–34], as was analyzed in detail by many theoretical works (see, e.g., [93–95], as well as [74, 96] and Chap. 2 for relevant reviews).

1.4.3 Macroscopic Excitations: Solitons and Vortices

Aside from the simpler states discussed above, strongly nonlinear and localized states have been observed experimentally in BECs by using various relevant techniques. These include phase engineering of the condensates in order to create vortices [97, 98] or dark matter-wave solitons in them [99–102] (see also Part III), the stirring (or rotation) of the condensates providing angular momentum and creating vortices [103, 104] (see also Part VI) and vortex-lattices [105–107] (see also Part VII), the change of scattering length (from repulsive to attractive via Feshbach resonances) to produce bright matter-wave solitons and soliton trains [32–34] in attractive condensates (see also Part II), or set into motion a repulsive BEC trapped in optical lattice to create gap matter-wave solitons [70] (see also Part IV). Both matter-wave solitons and vortices can be viewed as fundamental nonlinear excitations of the BECs, and as such have attracted considerable attention. As far as vortices and vortex lattices are concerned, it should be noted that their description and connection to phenomena as rich and profound as superconductivity and superfluidity, were one of the themes of the Nobel prize in Physics in 2003.

The main scope of the present book is to focus on such nonlinear phenomena and structures, emerging from the effective mean-field nonlinearity of BECs and to offer a review of the large volume of recent literature that has developed over the last decade in this forefront of research, interfacing between atomic, nonlinear and wave physics. Although the aforementioned nonlinear structures (i.e., the solitons and vortices) will thoroughly be discussed in the following chapters, it is worth closing this introductory chapter by briefly presenting the most fundamental ones, namely the bright and dark matter-wave solitons in 1D, as well as vortices in 2D. This way, we believe that it will be easier for the reader to follow the topical reviews that will be presented in the following chapters.

Let us again consider the dimensionless Gross–Pitaevskii (1.13). In the absence of the external potential, this equation becomes the "traditional" completely integrable NLS equation, which possesses different types of soliton solutions, depending on the parameter g. In particular, for *attractive* BECs

($g = -1$) the NLS equation possesses a *bright* soliton solution of the following form [108],

$$\psi(z,t) = \eta \,\mathrm{sech}[\eta(z - vt)] \exp[\mathrm{i}(kz - \omega t)], \tag{1.24}$$

where η is the amplitude and inverse spatial width of the soliton, k is the soliton wavenumber, $\omega = \frac{1}{2}(k^2 - \eta^2)$ is the soliton frequency, and $v \equiv \partial\omega/\partial k = k$ is the soliton velocity. The bright soliton (1.24) is characterized by *two* independent parameters. Note that the "soliton dispersion relation" $\omega = \frac{1}{2}(k^2 - \eta^2)$ implies that $\omega < \frac{1}{2}k^2$, and, hence, the allowable region in the (k, ω) plane for bright solitons is located *below* the parabola $\omega = \frac{1}{2}k^2$, corresponding to the elementary excitations (linear waves) of the NLS equation. The bright soliton solution is shown in Fig. 1.1a for $\eta = 1$ and $v = 3$.

On the other hand, in the *repulsive* BEC case ($g = +1$), the NLS equation possesses a dark soliton solution [109], which can be considered as an excitation of the plane wave solution $\psi = \psi_0 \exp[\mathrm{i}(kz - \omega t)]$. In particular, on a homogeneous background density ψ_0^2, the dark soliton may be expressed (in the most general case of a moving background) as [109],

$$\psi(z,t) = \psi_0 \left(\cos\varphi \tanh\zeta + \mathrm{i}\sin\varphi\right) \exp[\mathrm{i}(kz - \omega t)], \tag{1.25}$$

where $\zeta \equiv \psi_0 \cos\varphi\,(z - vt)$, the parameter $\omega = (1/2)k^2 + \psi_0^2$ characterizes the dispersion relation of the background plane wave, while the remaining

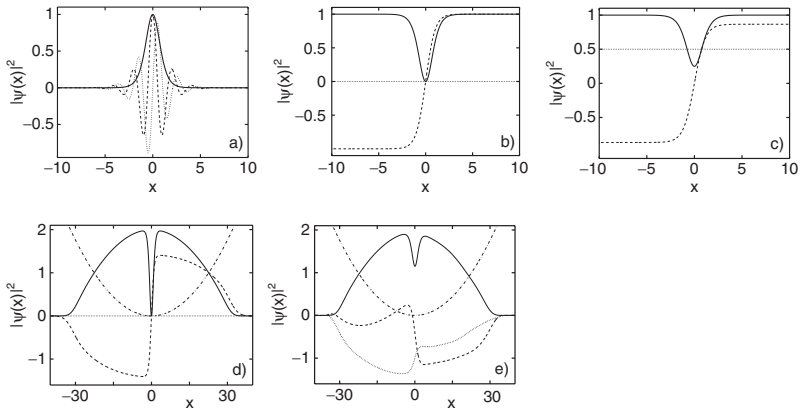

Fig. 1.1. One-dimensional excitations of the Gross–Pitaevskii equation. (**a**) Bright soliton in the absence of external potential with height $\eta = 1$ and velocity $v = 3$. (**b**) Stationary ($v = 0$) dark soliton in the absence of external potential with $k = 0$, $\mu = \psi_0^2 = 1$, $\varphi = 0$, and $\omega = 0$. (**c**) Moving gray soliton in the absence of external potential with $k = 0$, $\mu = \psi_0^2 = 1$, $v = 0.5$, $\varphi = \pi/6$, and $\omega = 1$. (**d**) Stationary ($v = 0$) dark soliton inside a magnetic trap with $\Omega = 1/16$ and $\mu = 2$. (**e**) Moving gray soliton inside a magnetic trap with $\Omega = 1/16$ and $\mu = 2$. In all panels the atomic density $|\psi(x)|^2$ is depicted by the *thick solid line* while the real and imaginary parts of the wavefunction are depicted with *thin dashed and dotted lines*, respectively. The magnetic external potential in (**e**) and (**d**) is depicted by the *thick dashed-dotted line*

soliton and background parameters, v, φ and k, are connected through the relation $v = \psi_0 \sin\varphi + k$. Here, φ is the so-called *soliton phase angle*, or, simply, the phase shift of the dark soliton ($|\varphi| < \pi/2$), which describes the *darkness* of the soliton through the relation, $|\psi|^2 = 1 - \cos^2\varphi \mathrm{sech}^2\zeta$; this way, the limiting cases $\varphi = 0$ and $\cos\varphi \ll 1$ correspond to the so-called *black* and *gray* solitons, respectively. Note that the amplitude and velocity of the dark soliton are given by $\cos\varphi$ and $\sin\varphi$ respectively; thus, the black soliton, $\psi = \psi_0 \tanh(\psi_0 x)\exp(-\mathrm{i}\mu t)$, is a stationary dark soliton ($v = 0$), while the gray soliton moves with a velocity close to the speed of sound ($v \sim \psi_0$). Apparently, the dark soliton solution (1.25) has three independent parameters, two for the background (ψ_0 and k) and one for the soliton (φ). Also, it should be noted that as in this case the dispersion relation implies that $\omega > k^2$, the allowable region in the (k, ω) plane for dark solitons is located *above* the parabola $\omega = \frac{1}{2}k^2$.

Usually, dark matter-wave solitons are considered in the simpler case where the background is at rest, i.e., $k = 0$; then, the frequency ω actually plays the role of a normalized one-dimensional chemical potential, namely $\mu \equiv \psi_0^2$, which is determined by the number of atoms of the condensate. Examples of such dark solitons, in the absence of external potential, are depicted in Fig 1.1b, c corresponding, respectively, to a quiescent, $v = 0$, dark soliton and a moving, $v = 0.5$, gray soliton. Moreover, it should be mentioned that in the case of an harmonically confined condensate, i.e., for $V(z) = \frac{1}{2}\Omega^2 z^2$ (Ω being the normalized trap strength) in (1.13), the background of the dark soliton can be approximated by the Thomas–Fermi cloud, $\psi_{\mathrm{TF}}(z) = \sqrt{\mu - V(x)}$ [see (1.19)]; thus, the "composite" wavefunction (containing both the Thomas–Fermi background and the dark soliton) takes the approximate form $\psi = \psi_{\mathrm{TF}}(z)\exp(-i\psi_0^2 t)\psi_{\mathrm{DS}}(z,t)$, where $\psi_{\mathrm{DS}}(z,t)$ is the dark soliton of (1.25). Examples of such a states are shown in Fig 1.1d, e corresponding, respectively, to a quiescent dark soliton and a moving gray soliton with $\Omega = 1/16$ and $\mu = 2$.

In the higher-dimensional setting, the NLS equation is no longer integrable. However, in the simplest 2D circularly symmetric setting, and for the repulsive BEC case ($g = +1$), stationary states with a phase singularity are possible. In the case of a homogeneous condensate ($\Omega = 0$), these states have the form $\psi(r,\theta,z) = \psi_0 U(r)\exp(\mathrm{i}m\theta - \mathrm{i}\psi_0^2 t)$, where r and θ are the polar coordinates, ψ_0 is the background density, and the integer m is the so-called *winding number* or *vortex charge*. These vortex states are the higher-dimensional analogues of black solitons (with the circular symmetry), and satisfy the following boundary value problem (for $\psi_0 = 1$),

$$\frac{\mathrm{d}^2 U}{\mathrm{d}r^2} + \frac{1}{r}\frac{\mathrm{d}U}{\mathrm{d}r} - \frac{m^2}{r^2}U + (1 - U^2)U = 0 \tag{1.26}$$

(resulting from (1.13) with ∂_z^2 being substituted by the 2D Laplacian), for $r > 0$ and the boundary conditions $U(0) = 0$ and $U(+\infty) = 1$. The asymptotic behavior of the vortex profile $U(r)$ can be found from (1.26), i.e., $U(r) \sim r^{|m|}$

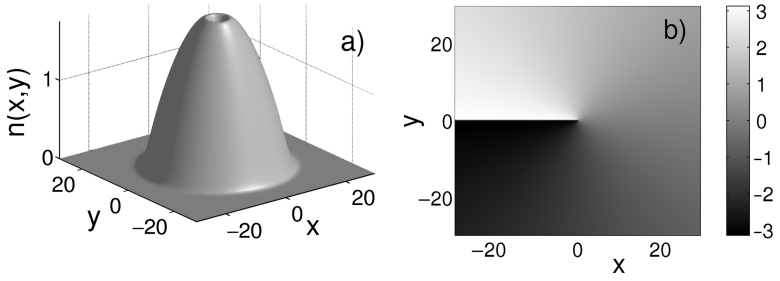

Fig. 1.2. Two-dimensional, singly charged ($m = 1$), vortex inside a magnetic trap with $\Omega = 0.1$. Depicted are (**a**) the density and (**b**) its phase profile for $\mu = 2$

as $r \to 0$, and $U(r) \sim 1 - \frac{m^2}{2r^2}$ as $r \to +\infty$. Similarly to the case of a dark soliton, a vortex in a condensate confined in the harmonic potential $V(r) = \frac{1}{2}\Omega^2 r^2$ is on top of the ground state profile which can be approximated by $\psi_{\rm TF}(r) = \sqrt{\mu - V(r)}$; thus, in this case, the wavefunction can by approximated by $\psi = \psi_{\rm TF}(r)U(r)\exp(\mathrm{i}m\theta - \mathrm{i}t)$. An example of such a vortex is shown in Fig. 1.2 for $\Omega = 0.1$, $m = 1$ and $\mu = 2$.

References

1. S.N. Bose, Z. Phys. **26**, 178 (1924)
2. A. Einstein, Sitzungsber. K. Preuss. Akad. Wiss., Phys. Math. Kl. **261** (1924)
3. A. Einstein, Sitzungsber. K. Preuss. Akad. Wiss., Phys. Math. Kl. **3** (1925)
4. A. Griffin, D.W. Snoke, S. Stringari (eds.), *Bose–Einstein Condensation* (Cambridge University Press, Cambridge, 1995)
5. M.H.J. Anderson, J.R. Ensher, M.R. Matthews, C.E. Wieman, Science **269**, 198 (1995)
6. K.B. Davis, M.-O. Mewes, M.R. Andrews, N.J. van Druten, D.S. Durfee, D.M. Kurn, W. Ketterle, Phys. Rev. Lett. **75**, 3969 (1995)
7. C.C. Bradley, C.A. Sackett, J.J. Tollett, R.G. Hulet, Phys. Rev. Lett. **75**, 1687 (1995)
8. See, e.g., C.C. Bradley, C.A. Sackett, J.J. Tollett, R.G. Hulet, Phys. Rev. Lett. **79**, 1170 (1997), and references therein
9. E.A. Cornell, C.E. Wieman, Rev. Mod. Phys. **74**, 875 (2002)
10. W. Ketterle, Rev. Mod. Phys. **74**, 1131 (2002)
11. E.P. Gross, J. Math. Phys. **4**, 195 (1963)
12. L.P. Pitaevskii, Sov. Phys. JETP **13**, 451 (1961)
13. C. Sulem, P.L. Sulem, *The Nonlinear Schrödinger Equation* (Springer, Berlin Heidelberg New York, 1999)
14. M.J. Ablowitz, B. Prinari, A.D. Trubatch, *Discrete and Continuous Nonlinear Schrödinger Systems* (Cambridge University Press, Cambridge, 2004)
15. J. Bourgain, *Global Solutions of Nonlinear Schrödinger Equations*, (American Mathematical Society, Providence, 1999)
16. F. Dalfovo, S. Giorgini, L.P. Pitaevskii, S. Stringari, Rev. Mod. Phys. **71**, 463 (1999)
17. L.P. Pitaevskii, S. Stringari, *Bose Einstein Condensation* (Clarendon Press Oxford, 2003)

18. C.J. Pethick, H. Smith, *Bose Einstein Condensation in Dilute Gases* (Cambridge University Press, Cambridge, 2004)
19. N.N. Bogoliubov, J. Phys. (Moscow) **11**, 23 (1947)
20. A.J. Leggett, Rev. Mod. Phys. **73**, 307 (2001)
21. Yu.S. Kivshar, G.P. Agrawal, *Optical Solitons: From Fibers to Photonic Crystals* (Academic, New York, 2003)
22. J. Weiner, *Cold and Ultracold Collisions in Quantum Microscopic and Mesoscopic Systems* (Cambridge University Press, Cambridge, 2003)
23. S. Inouye M.R. Andrews, J. Stenger, H.J. Miesner, D.M. Stamper-Kurn, W. Ketterle, Nature **392**, 151 (1998)
24. J. Stenger, S. Inouye, M.R. Andrews, H.-J. Miesner, D.M. Stamper-Kurn, W. Ketterle, Phys. Rev. Lett. **82**, 2422 (1999)
25. J.L. Roberts, N.R. Claussen, J.P. Burke, Jr., C.H. Greene, E.A. Cornell, C.E. Wieman , Phys. Rev. Lett. **81**, 5109 (1998)
26. S.L. Cornish, N.R. Claussen, J.L. Roberts, E.A. Cornell, C.E. Wieman, Phys. Rev. Lett. **85**, 1795 (2000)
27. A.J. Moerdijk, B.J. Verhaar, A. Axelsson, Phys. Rev. A **51**, 4852 (1995)
28. J.L. Roberts, N.R. Claussen, S.L. Cornish, C.E. Wieman, Phys. Rev. Lett. **85**, 728 (2000)
29. M. Olshanii, Phys. Rev. Lett. **81**, 938 (1998)
30. T. Bergeman, M.G. Moore, M. Olshanii, Phys. Rev. Lett. **91**, 163201 (2003)
31. M. Theis, G. Thalhammer, K. Winkler, M. Hellwig, G. Ruff, R. Grimm, J.H. Denschlag, Phys. Rev. Lett. **93**, 123001 (2004)
32. K.E. Strecker, G.B. Partridge, A.G. Truscott, R.G. Hulet, Nature **417** 150 (2002)
33. L. Khaykovich, F. Schreck, G. Ferrari, T. Bourdel, J. Cubizolles, L.D. Carr, Y. Castin, C. Salomon, Science, **296** 1290 (2002)
34. S.L. Cornish, S.T. Thompson, C.E. Wieman, Phys. Rev. Lett. **96**, 170401 (2006)
35. K.E. Strecker, G.B. Partridge, A.G. Truscott, R.G. Hulet, New J. Phys. **5**, 73 (2003)
36. J. Herbig, T. Kraemer, M. Mark, T. Weber, C. Chin, H.C. Nagerl, R. Grimm, Science **301**, 1510 (2003)
37. C.A. Regal, C. Ticknor, J.L. Bohn, D.S. Jin, Nature **424**, 47 (2003)
38. M. Greiner, C.A. Regal, D.S. Jin, Nature **426**, 537 (2003)
39. M. Bartenstein, A. Altmeyer, S. Riedl, S. Jochim, C. Chin, J.H. Denschlang, R. Grimm, Phys. Rev. Lett. **92**, 203201 (2004)
40. T. Bourdel, L. Khaykovich, J. Cubizolles, J. Zhang, F. Chevy, M. Teichmann, L. Tarruell, S.J.J.M.F. Kokkelmans, C. Salomon, Phys. Rev. Lett. **93**, 050401 (2004)
41. D.M. Stamper-Kurn, M.R. Andrews, A.P. Chikkatur, S. Inouye, H.J. Miesner, J. Stenger, W. Ketterle, Phys. Rev. Lett. **80**, 2027 (1998)
42. J. Weiner, V.S. Bagnato, S. Zilio, P.S. Julienne, Rev. Mod. Phys. **71**, 1 (1999)
43. R. Grimm, M. Weidemüller, Y.B. Ovchinnikov, Adv. At. Mol. Opt. Phys. **42**, 95 (2000)
44. M.D. Barrett, J.A. Sauer, M.S. Chapman, Phys. Rev. Lett. **87**, 010404 (2001)
45. P.S. Jessen, C. Gerz, P.D. Lett, W.D. Phillips, S.L. Rolston, R.J.C. Spreeuw, C.I. Westbrook, Phys. Rev. Lett. **69**, 49 (1992)
46. P. Verkerk, B. Lounis, C. Salomon, C. Cohen-Tanoudji, J.Y. Courtois, G. Grynberg, Phys. Rev. Lett. **68**, 3861 (1992)

47. B.P. Anderson, T.I. Gustavson, M.I. Kasevich, Phys. Rev. A **53**, R3727 (1996)
48. O. Morsch, M.K. Oberthaler, Rev. Mod. Phys. **78**, 179 (2006)
49. A. Görlitz, J.M. Vogels, A.E. Leanhardt, C. Raman, T.L. Gustavson, J.R. Abo-Shaeer, A.P. Chikkatur, S. Gupta, S. Inouye, T. Rosenband, W. Ketterle, Phys. Rev. Lett. **87**, 130402 (2001)
50. M. Greiner, I. Bloch, O. Mandel, T.W. Hänsch, T. Esslinger, Phys. Rev. Lett. **87**, 160405 (2001)
51. S. Burger, F.S. Cataliotti, C. Fort, P. Maddaloni, F. Minardi, M. Inguscio, Europhys. Lett. **57**, 1 (2002)
52. H. Moritz, T. Stöferle, M. Köhl, T. Esslinger, Phys. Rev. Lett. **91**, 250402 (2003)
53. F.S. Cataliotti, S. Burger, C. Fort, P. Maddaloni, F. Minardi, A. Trombettoni, A. Smerzi, M. Inguscio, Science **293**, 843 (2001)
54. S. Burger, F.S. Cataliotti, C. Fort, F. Minardi, M. Inguscio, M.L. Chiofalo, M.P. Tosi, Phys. Rev. Lett. **80**, 4447 (2001)
55. J.H. Denschlag, J.E. Simsarian, H. Haffner, C. McKenzie, A. Browaeys, D. Cho, K. Helmerson, S.L. Rolston, W.D. Phillips, J. Phys. B **35**, 3095 (2002)
56. W. Hänsel, P. Hommelhoff, T.W. Hänsch, J. Reichel, Nature (London) **413**, 501 (2001)
57. H. Ott, J. Fortagh, G. Schlotterbeck, A. Grossmann, C. Zimmermann, Phys. Rev. Lett. **87**, 230401 (2001)
58. E.H. Lieb, R. Seiringer, J.P. Solovej, J. Yngvason, *The Mathematics of the Bose Gas and its Condensation*. Oberwolfach Seminar Series, vol 34 (Birkhaeuser, Basel 2005) (arXiv:cond-mat/0610117)
59. L. Tonks, Phys. Rev. **50**, 955 (1936)
60. M. Girardeau, J. Math. Phys. (N.Y.) **1**, 516 (1960)
61. B. Paredes, A. Widera, V. Murg, O. Mandel, S. Folling, I. Cirac, G.V. Shlyapnikov, T.W. Häansch, I. Bloch, Nature **429**, 277 (2004)
62. T. Kinoshita, T. Wenger, D.S. Weiss, Science **305**, 1125 (2004)
63. O. Morsch, E. Arimondo, in ed. by T. Dauxois, S. Ruffo, E. Arimondo, M. Wilkens Dynamics and Thermodynamics of Systems with Long-Range Interactions, (Springer, Berlin, 2002), p. 312
64. S. Peil, J.V. Porto, B.L. Tolra, J.M. Obrecht, B.E. King, M. Subbotin, S.L. Rolston, W.D. Phillips, Phys. Rev. A **67**, 051603(R) (2003)
65. M.R. Andrews, C.G. Townsend, H.-J. Miesner, D.S. Durfee, D.M. Kurn, W. Ketterle, Science **275**, 637 (1999)
66. M. Albiez, R. Gati, J. Fölling, S. Hunsmann, M. Cristiani, M.K. Oberthaler, Phys. Rev. Lett. **95**, 010402 (2005)
67. B.P. Anderson, M.A. Kasevich, Science **282**, 1686 (1998)
68. R. Folman, J. Schmiedmayer, Nature **413**, 466 (2001)
69. R. Folman, P. Krueger, J. Schmiedmayer, J. Denschlag, C. Henkel, Adv. Atom. Mol. Opt. Phys. **48**, 263 (2002)
70. B. Eiermann, Th. Anker, M. Albiez, M. Taglieber, P. Treutlein, K.P. Marzlin, M.K. Oberthaler, Phys. Rev. Lett. **92**, 230401 (2004)
71. V.M. Pérez-García, H. Michinel, H. Herrero, Phys. Rev. A **57**, 3837 (1998)
72. A.D. Jackson, G.M. Kavoulakis, C.J. Pethick, Phys. Rev. A **58**, 2417 (1998)
73. Yu.S. Kivshar, T.J. Alexander, S.K. Turitsyn, Phys. Lett. A **278**, 225 (2001)
74. F.Kh. Abdullaev, A. Gammal, A.M. Kamchatnov, L. Tomio, Int. J. Mod. Phys. B **19**, 3415 (2005)

75. V.V. Konotop, M. Salerno, Phys. Rev. A **65**, 021602 (2002)
76. F.Kh. Abdullaev, A.M. Kamchatnov, V.V. Konotop, V.A. Brazhnyi, Phys. Rev. Lett. **90**, 230402 (2003)
77. L. Salasnich, A. Parola, L. Reatto, Phys. Rev. A **65**, 043614 (2002)
78. Y.B. Band, I. Towers, B.A. Malomed, Phys. Rev. A **67**, 023602 (2003)
79. Yu. Kagan, A.E. Muryshev, G.V. Shlyapnikov, Phys. Rev. Lett. **81**, 933 (1988)
80. F.Kh. Abdullaev, A. Gammal, L. Tomio, T. Frederico, Phys. Rev. A **63**, 043604 (2001)
81. A.E. Muryshev, G.V. Shlyapnikov, W. Ertmer, K. Sengstock, M. Lewenstein, Phys. Rev. Lett. **89**, 110401 (2002)
82. L. Khaykovich, B.A. Malomed, Phys. Rev. A **74**, 023607 (2006)
83. P.G. Kevrekidis, K.Ø. Rasmussen, A.R. Bishop, Int. J. Mod. Phys. B, **15**, 2833 (2001)
84. A. Trombettoni, A. Smerzi, Phys. Rev. Lett. **86**, 2353 (2001)
85. F.Kh. Abdullaev, B.B. Baizakov, S.A. Darmanyan, V.V. Konotop, M. Salerno, Phys. Rev. A **64**, 043606 (2001)
86. E.G. Alfimov, P.G. Kevrekidis, V.V. Konotop, M. Salerno, Phys. Rev. E **66**, 046608 (2002)
87. W. Kohn, Phys. Rev. **115**, 809 (1959)
88. J.M. Gerton, D. Strekalov, I. Prodan, R.G. Hulet, Nature **408**, 692 (2000)
89. E.A. Donley, N.R. Claussen, S.L. Cornish, J.L. Roberts, E.A. Cornell, C.E. Wieman, Nature, **412**, 295 (2001)
90. P.A. Ruprecht, M.J. Holland, K. Burnett, C.W. Clark, Phys. Rev. A **51**, 4704 (1995)
91. A. Gammal, T. Frederico, L. Tomio, Phys. Rev. A **64**, 055602 (2001)
92. A. Gammal, T. Frederico, L. Tomio, Phys. Rev. A **66**, 043619 (2002)
93. G. Theocharis, Z. Rapti, P.G. Kevrekidis, D.J. Frantzeskakis, V.V. Konotop, Phys. Rev. A **67**, 063610 (2003)
94. L. Salasnich, A. Parola, L. Reatto, Phys. Rev. Lett. **91**, 80405 (2003)
95. L.D. Carr, J. Brand, Phys. Rev. A **70**, 033607 (2004)
96. P.G. Kevrekidis, D.J. Frantzeskakis, Mod. Phys. Lett. B **18**, 173 (2004)
97. M.R. Matthews, B.P. Anderson, P.C. Haljan, D.S. Hall, C.E. Wieman, E.A. Cornell, Phys. Rev. Lett. **83**, 2498 (1999)
98. J.E. Williams, M.J. Holand, Nature **568**, 401 (1999)
99. J. Denschlag, J.E. Simsarian, D.L. Feder, C.W. Clark, L.A. Collins, J. Cubizolles, L. Deng, E.W. Hagley, K. Helmerson, W.P. Reinhardt, S.L. Rolston, B.I. Schneider, W.D. Phillips, Science, **287**, 97 (2000)
100. S. Burger, K. Bongs, S. Dettmer, W. Ertmer, K. Sengstock, A. Sanpera, G.V. Shlyapnikov, M. Lewenstein, Phys. Rev. Lett. **83**, 5198 (1999)
101. B.P. Anderson, P.C. Haljan, C.A. Regal, D.L. Feder, L.A. Collins, C.W. Clark, E.A. Cornell, Phys. Rev. Lett. **86**, 2926 (2001)
102. Z. Dutton, M. Budde, C. Slowe, L.V. Hau, Science **293**, 663 (2001)
103. K.W. Madison, F. Chevy, W. Wohlleben, J. Dalibard, Phys. Rev. Lett. **84**, 806 (1999)
104. S. Inouye, S. Gupta, T. Rosenband, A.P. Chikkatur, A. Görlitz, T.L. Gustavson, A.E. Leanhardt, D.E. Pritchard, W. Ketterle, Phys. Rev. Lett. **87**, 080402 (2001)
105. J.R. Abo-Shaeer, C. Raman, J.M. Vogels, W. Ketterle, Science **292**, 476 (2001)
106. J.R. Abo-Shaeer, C. Raman, W. Ketterle, Phys. Rev. Lett. **88**, 070409 (2002)

107. P. Engels, I. Coddington, P.C. Haljan, E.A. Cornell, Phys. Rev. Lett. **89**, 100403 (2002)
108. V.E. Zakharov, A.B. Shabat, Zh. Eksp. Teor. Fiz. **61**, 118 (1971) [Sov. Phys. JETP **34**, 62 (1971)]
109. V.E. Zakharov, A.B. Shabat, Zh. Eksp. Teor. Fiz. **64**, 1627 (1973) [Sov. Phys. JETP **37**, 823 (1973)]

Springer

http://www.springer.com/978-3-540-73590-8

Emergent Nonlinear Phenomena in Bose-Einstein Condensates

Theory and Experiment

Kevrekidis, P.G.; Frantzeskakis, D.J.; Carretero-González, R. (Eds.)

2008, XXII, 405 p., Hardcover
ISBN: 978-3-540-73590-8